

## Dynamics and excitations of a solvated electron in molecular clusters

R. N. Barnett and Uzi Landman

*School of Physics, Georgia Institute of Technology, Atlanta, Georgia 30332*

Abraham Nitzan

*School of Chemistry, Tel Aviv University, 69 978 Tel Aviv, Israel*

(Received 10 August 1987)

A method for investigations of the ground and excited states and the dynamical evolution of coupled quantum-classical systems is presented. A time-dependent self-consistent-field procedure is used where the time evolution of the wave function is evaluated with use of fast Fourier transforms and the coupled classical motion is treated via classical molecular dynamics. Different modes of simulations are demonstrated for electron attachment to NaCl and water clusters.

Quantum-mechanical Monte Carlo and molecular-dynamics simulations of the equilibrium state of a solvated electron in noble and polar fluids (water, ammonia, and molten KCl) have been recently carried out using the isomorphic classical chain representation of the path-integral expression for the quantum partition function.<sup>1</sup> Quantum path-integral molecular dynamics (QUPID) simulations were also carried out for alkali halide<sup>2</sup> and water and ammonia clusters,<sup>3</sup> yielding new information on the structure, energetics, isomerization, and mode of electron attachment to these clusters, at thermal equilibrium. There have also been several attempts<sup>1,4</sup> to generalize this method to the real time domain.

In this paper we present an alternative approach for investigations of dynamical and equilibrium processes in systems characterized by coupled quantum-mechanical and classical components. The method is based on a time-dependent self-consistent-field<sup>5</sup> (TDSCF) hybridiza-

tion of the fast-Fourier-transform (FFT) technique<sup>6</sup> for the solution of the time-dependent Schrödinger equation with classical molecular-dynamics (MD) evolution.<sup>7,8</sup> The method handles effectively situations of large time-scale separation between the quantum-mechanical and classical evolutions which would normally make such computations prohibitively long. Furthermore, the method yields excited-state energies, including resonances above the ionization threshold. We discuss the method and different modes of its use and demonstrate it via studies of the ground- and excited-states energetics and dynamics of an electron solvated in molecular clusters.

The quantum time evolution in the FFT method is based<sup>6</sup> on a repeated evaluation of the short-time propagation of the wave function (in real or imaginary time) according to

$$\psi(\mathbf{r}, t + \Delta t) = \exp \left[ -\frac{i}{\hbar} (\hat{K} + \hat{V}) \Delta t \right] \psi(\mathbf{r}, t) = \exp \left[ -\frac{1}{2} \frac{i}{\hbar} \hat{K} \Delta t \right] \exp \left[ -\frac{i}{\hbar} \hat{V} \Delta t \right] \exp \left[ -\frac{1}{2} \frac{i}{\hbar} \hat{K} \Delta t \right] \psi(\mathbf{r}, t) + O((\Delta t)^3), \quad (1)$$

where  $\hat{K}$  and  $\hat{V}$  are the kinetic and potential-energy operators, and an expansion in the plane-wave, free-particle, basis set

$$\psi(\mathbf{r}, t + \Delta t) = \frac{1}{(2\pi)^3} \exp \left[ -\frac{i}{2\hbar} \hat{K} \Delta t \right] \exp \left[ -\frac{i}{\hbar} V(\mathbf{r}) \Delta t \right] \int d^3k e^{i\mathbf{k}\cdot\mathbf{r}} \exp \left[ -\frac{i\hbar k^2}{4m} \Delta t \right] \int d^3r' e^{-i\mathbf{k}\cdot\mathbf{r}'} \psi(\mathbf{r}', t), \quad (2)$$

where  $m$  is the mass of the particle. The FFT algorithm is applied to the discretized version of Eq. (2). The coupling between the quantum and classical (denoted collectively by the coordinates and masses  $\{\mathbf{r}_c\}$  and  $\{m_c\}$ ) subsystems is described within the TDSCF approximation

$$\frac{\partial \psi(\mathbf{r}, t)}{\partial t} = -\frac{i}{\hbar} H(\mathbf{r}, \{\mathbf{r}_c\}) \psi(\mathbf{r}, t), \quad (3)$$

$$m_c \ddot{\mathbf{r}}_c = -\frac{\partial}{\partial \mathbf{r}_c} \left[ \int d\mathbf{r} V(\mathbf{r}, \{\mathbf{r}_c\}) |\psi(\mathbf{r}, t)|^2 + U(\{\mathbf{r}_c\}) \right], \quad (4)$$

where  $H(\mathbf{r}, \{\mathbf{r}_c\}) = H_0(\mathbf{r}) + V(\mathbf{r}, \{\mathbf{r}_c\}) + U(\{\mathbf{r}_c\})$ ,  $H_0$  is

the Hamiltonian of the isolated quantum particle,  $V$  is the quantum-classical interaction potential, and  $U$  is the interaction between the classical particles. In this approximation the classical system moves in the quantum-averaged interaction potential  $\langle V \rangle$  [integral on the right-hand side of Eq. (4)] and the classical interaction,  $U(\{\mathbf{r}_c\})$ .

The method can be used in three different modes: (a) evaluation of the time-dependent wave functions  $\psi(t)$  for an arbitrary initial state  $\psi(0)$  for a fixed configuration of the classical subsystem, yielding the energy eigenvalues as the positions of peaks in the time Fourier transform of the correlation function

$$C(t) = \langle \psi(0) | \psi(t) \rangle = \sum_n \langle \psi(0) | \psi_n \rangle e^{-iE_n t / \hbar}$$

( $E_n$  and  $\psi_n$  are the corresponding eigenvalues and eigenfunctions). The ground-state energy and wave function can be also obtained by evolving an arbitrary initial wave function in imaginary time until convergence. (b) For systems where a large separation between the electron ground and excited states restricts the nuclear dynamics (at moderate temperatures) to the (adiabatic) ground-state electronic potential-energy surface, the dynamics can be followed by evolving the classical system in real time while *simultaneously* "quenching" the electronic wave function to the ground state corresponding to the instantaneous nuclear configuration by evolving it in imaginary time with  $e^{-\beta \hat{H}}$ , where  $\beta \rightarrow \infty$ , followed by normalization. This mode, which we term *ground-state dynamics* (GSD), is very effective in systems where the large time-scale separation between the nuclear and electronic motions makes the full dynamical simulation for both subsystems both unnecessary (since the adiabatic approximation holds) and costly. (c) When the separation of electronic energy levels is not very large relative to the classical (nuclear) energies, full dynamics within the TDSCF approximation is obtained.<sup>9</sup> The results presented below demonstrate the use of these different modes.

Figure 1(b) shows the eigenstate spectrum of the  $(\text{NaCl})^-$  molecular anion obtained as the time Fourier transform  $I(E)$  of  $\langle \psi(0) | \psi(t) \rangle$ . In this calculation the neutral nuclei are static at their equilibrium position<sup>10</sup>  $R_{\text{Cl-Na}} = 4.74a_0$  and we have used the  $e\text{-Na}^+$  and  $e\text{-Cl}^-$  potentials discussed earlier.<sup>10</sup> The height of the peaks has no physical significance and reflects the (arbitrary) choice of the initial wave function. The peak positions show a bound-state energy of  $-0.04$  hartree (in good agreement with QUPID calculations<sup>10</sup>) and several resonance states,

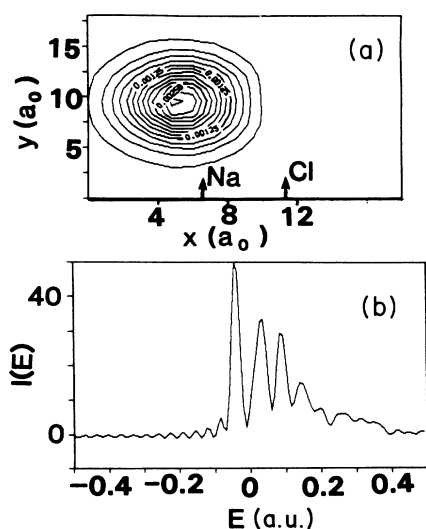


FIG. 1. (a) Contours of the excess electron density corresponding to the ground-state wave function in the plane containing the nuclei whose equilibrium locations are denoted. (b) Fourier transform,  $I(E)$  in arbitrary units, of the correlation function  $\langle \psi(0) | \psi(t) \rangle$  for  $\text{NaCl}^-$  showing a bound state at  $-0.04$  a.u. and several resonances. (1 a.u. = 2 Rydbergs.)

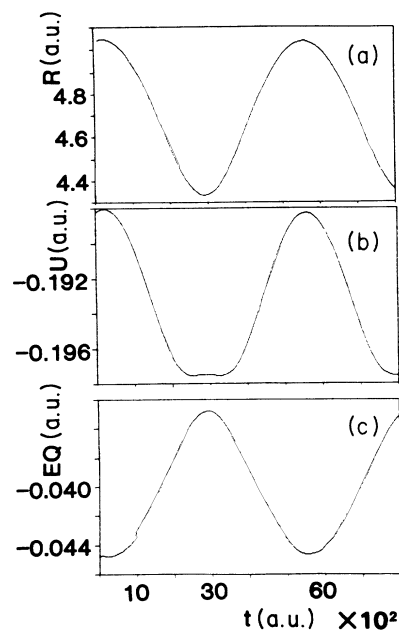


FIG. 2. Dynamics of the internuclear distance  $R$ , interionic potential energy  $U$ , and energy of the electron  $EQ$ , (a), (b), and (c), respectively, for  $\text{NaCl}^-$  at 50 K. Time in a.u. =  $2.4189 \times 10^{-17}$  sec.

the lowest of which is at 0.03 hartrees above zero.

More detailed information about the structure of the ground electronic state is obtained by using the  $e^{-\beta \hat{H}}$  ( $\beta \rightarrow \infty$ ) operation. In practice, we find that convergence is very fast, provided that the ground state is not nearly degenerate. This yields (after normalization) the ground-state wave function, shown in Fig. 1(a) from which we calculate  $\langle KQ \rangle = 0.046$ ,  $\langle V \rangle = -0.0866$  hartree, and  $\langle (r - \langle r \rangle)^2 \rangle^{1/2} = 5.4a_0$ , in agreement with the results obtained earlier<sup>10</sup> for this system.

We turn next to studies of electron attachment to water clusters  $(\text{H}_2\text{O})_n$  which have been investigated recently<sup>3</sup> using the QUPID method employing an electron-water pseudopotential<sup>3</sup> which includes Coulomb, polarization, exclusion, and exchange contributions. It was found<sup>3</sup> that the adiabatic electron affinity, which expresses the balance between the electron binding and the cluster molecular reorganization energies, favors the formation of surface states as the stable equilibrium configurations for cluster sizes  $n \lesssim 60$ , whereas for larger clusters an internal mode of localization is dominant. Furthermore, the calculated vertical electron affinities are in agreement with photoelectron data.<sup>11</sup> Using cluster nuclear configurations picked at random from the equilibrium ensembles generated via the QUPID calculations and the  $e\text{-H}_2\text{O}$  pseudopotential, we have applied mode (a) of the method, obtaining the *ground-* and *excited-*state energies.<sup>12</sup> In Table I the ground-state energies are summarized, averaged over four QUPID nuclear equilibrium configurations, along with the equilibrium-averaged QUPID results.<sup>3</sup> We first note the close agreement between the ground-state information obtained by the two methods. We have found that for clusters  $(\text{H}_2\text{O})_n^-$  with

$n \geq 8$  the ground-state energy (vertical binding energy) is only weakly sensitive to the (static) cluster configuration chosen. Excited-state energies can vary by as much as 10% for  $n < 32$ .

A strongly appealing feature of the FFT approach is the ability to get ground- and excited-state information from the same calculation. For  $(\text{H}_2\text{O})_n^-$  clusters with  $n = 32, 64,$  and  $128$  the first excited states are found [using mode (a)] at  $+0.035, -0.00875,$  and  $-0.04187$  hartrees, respectively. We observe that the first electronically excited state of the water cluster negative ion changes its nature from a resonance to a bound state for  $32 < n < 64$ . Secondly, we find that the first transition en-

ergy is red shifted as the cluster size increases ( $\Delta E = 0.1158, 0.0978,$  and  $0.0875$  hartrees for  $n = 32, 64,$  and  $128$ , respectively). Note that  $\Delta E = 0.0625$  hartrees (at the peak) for bulk water.<sup>13</sup> These results demonstrate the effect of long-range interactions on the electronic states (excited states, in particular) of the attached electron.

Results of a GSD calculation [mode (b)] for  $(\text{NaCl})^-$  are shown in Fig. 2. For this system the separation between the ground and excited electronic states is large enough ( $\sim 1$  eV) relative to the nuclear energies to disregard electronic excitation. The electron is therefore kept at its ground state by application of the  $\hat{N}e^{-\beta H}$  operation ( $\hat{N}$  is the normalization operator and  $\beta \rightarrow \infty$ ) repeatedly as the classical dynamics of the nuclei is evaluated. As evident from the figure, the electronic binding energy varies as the internuclear distance changes upon vibrations of the negative ion. The vibrational frequency of  $(\text{NaCl})^-$  [see Fig. 2(a)] is  $7.5 \times 10^{12} \text{ sec}^{-1}$  compared to the experimental value<sup>14</sup> of  $7.94 \times 10^{12} \text{ sec}^{-1}$ .

An extreme opposite case (i.e., nonseparable time scales for the electronic and nuclear motions) is that of the negative water dimer  $(\text{H}_2\text{O})_2^-$  where the excess electron binding energy ( $\sim 2 \times 10^{-14}$  hartree) is smaller than typical nuclear energies. Figure 3 depicts the results of a full dynamical calculation of this system [mode (c)] at a temperature  $T = 20$  K. (In calculations involving nuclear dynamics, constant-temperature molecular dynamics was used.<sup>3</sup>) The electron binding in this case is affected mostly by the total dipole of the water dimer (due to the diffuse nature of the electron cloud;<sup>3</sup> see Table I), which changes in time with the relative orientation of the two water molecules. The correlation between the nuclear motion and the electronic energies is clearly exhibited. While the potential energy of the classical system  $U$  [Fig. 3(a)], in the high-dipole nuclear configurations is larger than that in the low-dipole state, transitions into these configurations are enhanced by the increase in the magnitude of the electron binding energy [Fig. 3(d)].<sup>15</sup> The TDSCF method, where the nuclei move on the average electronic potential-energy surface (PES), is not applicable when nonadiabatic transitions occur and the PES's corresponding to the electron states involved differ greatly. For the dynamics of  $(\text{H}_2\text{O})_2^-$  this is not expected to be the case, since even if more than one electronic state is involved the corresponding average PES's should not depart significantly due to the extreme diffuseness of the excess electron distribution<sup>3</sup> (see Table I).

All the calculations reported above were done using  $16^3$  point grids (except for  $n = 2$  and  $8$  where the number of points was doubled). We verified that the results are insensitive (within 2–5%) to the grid distance parameter [typically chosen between 1 and 1.5 a.u., 9 a.u. for the  $(\text{H}_2\text{O})_2^-$  calculation]. The method yields results in good agreement with those of earlier calculations done by other methods. Furthermore, the method allows an efficient determination of excited-state spectra and investigations of dynamical evolution, at finite temperatures, of complex systems.

*Note added in proof.* In our recent studies<sup>16</sup> of the energetics and spectroscopy of  $(\text{H}_2\text{O})_n^-$  clusters we have

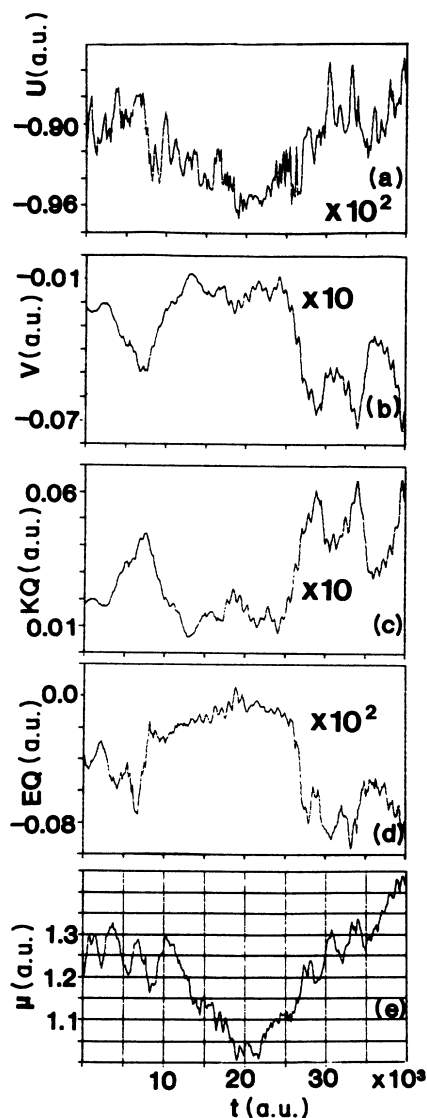


FIG. 3. Dynamics of  $(\text{H}_2\text{O})_2^-$ . The molecular potential-energy  $U$  interaction energy between the excess electron and the cluster  $V$ , kinetic energy of the electron  $(KQ)$ , total energy of the electron, and the magnitude of the total dipole of the water molecules are shown in (a)–(e), respectively. Time in a.u.  $= 2.4189 \times 10^{-17}$  sec. Note the correlation between the increases in the electron binding energy  $(EQ)$  and the cluster dipole, as the nuclear configuration fluctuates.

TABLE I. Ground-state energies calculated via the MD-TDSCF and QUPID methods, for  $(\text{H}_2\text{O})_n^-$  clusters.  $\langle V \rangle$ ,  $\langle KQ \rangle$ , and  $\langle EQ \rangle$  are the electron potential, kinetic, and total quantum binding energies, respectively, in hartrees.  $\langle R^2 \rangle^{1/2}$  is the electron-distribution radius of gyration in  $a_0$ . Temperatures in the QUPID calculations were  $n=2$  at 20 K;  $n=8, 12, 18$  at 79 K;  $n=32, 64, 128$  at 300 K. For  $n=2, 8, 12$  the electron attachment is via a surface state. For  $n=18$  both the surface ( $S$ ) and bulk ( $B$ ) states are given [the former possesses a higher adiabatic electron affinity (Ref. 3)]. For  $n=32, 64, 128$  the electron attachment is via bulk states. The MD-FFT results are averaged over four arbitrarily selected equilibrium configurations taken from the QUPID simulations. For  $n=2$  the molecular configuration is as in the neutral cluster.

| $(\text{H}_2\text{O})_n^-$ | $\langle V \rangle$ | $\langle KQ \rangle$ | $\langle EQ \rangle$ | $\langle R^2 \rangle^{1/2}$ |
|----------------------------|---------------------|----------------------|----------------------|-----------------------------|
| $n=2$                      | -0.000 83           | 0.000 67             | -0.000 16            | 56                          |
| QUPID                      | -0.0008             | 0.0007               | -0.0001              | 38                          |
| $n=8$                      | -0.0216             | 0.0137               | -0.0078              | 11.7                        |
| QUPID                      | -0.0212             | 0.0137               | -0.0074              | 11                          |
| $n=12$                     | -0.0666             | 0.0344               | -0.0323              | 6.9                         |
| QUPID                      | -0.0745             | 0.0382               | -0.0363              | 6                           |
| $n=18$ ( $S$ )             | -0.0839             | 0.0462               | -0.0377              | 5.9                         |
| QUPID                      | -0.0920             | 0.0438               | -0.0482              | 5.5                         |
| $n=18$ ( $B$ )             | -0.1486             | 0.0781               | -0.0705              | 4.2                         |
| QUPID                      | -0.1543             | 0.0823               | -0.0720              | 4.1                         |
| $n=32$                     | -0.1667             | 0.0859               | -0.0808              | 4.0                         |
| QUPID                      | -0.1778             | 0.0869               | -0.0908              | 3.8                         |
| $n=64$                     | -0.1930             | 0.0865               | -0.1065              | 4.0                         |
| QUPID                      | -0.2042             | 0.0866               | -0.1176              | 3.8                         |
| $n=128$                    | -0.2146             | 0.0852               | -0.1294              | 4.0                         |
| QUPID                      | -0.2169             | 0.0865               | -0.1304              | 3.9                         |

used the imaginary-time evolution, described under mode (b), for determination of ground-state energies, and in conjunction with a projection operator technique, for evaluation of successively higher excited states. GSD calculations in which the above method was implemented yield the following results for the ground, first excited-state, and transition energies, respectively (in hartrees): -0.1073, -0.0334, and 0.0745 for  $n=64$ ; -0.1399, -0.0612, and 0.0727 for  $n=128$ . These results are the

averages over long GSD trajectories and thus are more accurate than the values given in this paper which were obtained via mode (a) for a limited number of configurations.

This research was supported by U.S. Department of Energy Grant No. FG-05-86ER45234. Support by a Control Data Corporation Pacer grant to A.N. is acknowledged.

<sup>1</sup>For a review, see B. J. Berne and D. Thirumalai, *Ann. Rev. Phys. Chem.* **37**, 401 (1986), and references therein.

<sup>2</sup>U. Landman, D. Scharf, and J. Jortner, *Phys. Rev. Lett.* **54**, 1860 (1985); D. Scharf, U. Landman, and J. Jortner, *J. Chem. Phys.* **87**, 2716 (1987).

<sup>3</sup>R. N. Barnett, U. Landman, C. L. Cleveland, and J. Jortner, *Phys. Rev. Lett.* **59**, 811 (1987); U. Landman, R. N. Barnett, C. L. Cleveland, D. Scharf, and J. Jortner, *J. Phys. Chem.* **91**, 4890 (1987); R. N. Barnett, U. Landman, C. L. Cleveland, and J. Jortner, *J. Chem. Phys.* **88**, 4421 (1988); **88**, 4429 (1988); R. N. Barnett, U. Landman, C. L. Cleveland, N. R. Kestner, and J. Jortner, *ibid.* **88**, 6670 (1988).

<sup>4</sup>J. Chang and W. H. Miller, *J. Chem. Phys.* **87**, 1648 (1987); J. D. Doll, R. D. Colson, and D. L. Freeman, *ibid.* **87**, 1641 (1987).

<sup>5</sup>P. A. M. Dirac, *Proc. Cambridge Philos. Soc.* **26**, 376 (1930); D. Kumamoto and R. Silbey, *J. Chem. Phys.* **75**, 5164 (1981).

<sup>6</sup>M. D. Feit, J. A. Fleck, Jr., and A. Steiger, *J. Comput. Phys.* **47**, 412 (1982).

<sup>7</sup>Z. Kotler, A. Nitzan, and R. Kosloff, in *Tunneling*, edited by J. Jortner and B. Pullman (Reidel, Boston, 1986), p. 193.

<sup>8</sup>For a most recent application, see A. Selloni, P. Carnevali, R. Car, and M. Parinello, *Phys. Rev. Lett.* **59**, 823 (1987), Refs.

5-8 therein.

<sup>9</sup>Such a calculation was recently reported (Ref. 8) for an excess electron in a molten salt. For this system and others which satisfy the criterion for applicability for the GSD method, we recommend the use of that, more efficient, method rather than mode (c).

<sup>10</sup>D. Scharf, J. Jortner, and U. Landman, *Chem. Phys. Lett.* **130**, 504 (1986).

<sup>11</sup>J. V. Coe, D. R. Worsnop, and K. H. Bowen, *J. Chem. Phys.* (to be published).

<sup>12</sup>For recent calculations of an electron in liquid ammonia using rigid molecular configurations and employing simulated annealing, see M. Sprik and M. L. Klein, *J. Chem. Phys.* **87**, 5987 (1987).

<sup>13</sup>J. Jortner and R. M. Noyes, *J. Phys. Chem.* **70**, 770 (1966).

<sup>14</sup>T. M. Miller, D. G. Leopold, K. K. Murray, and W. C. Lineberger, *J. Chem. Phys.* **85**, 2368 (1986).

<sup>15</sup>A high-binding state ( $\sim 20$  meV) of  $(\text{H}_2\text{O})_2^-$  was also observed in our earlier QUPID calculations (see Landman *et al.*, Ref. 3). Recent measurements [K. Bowen (private communication)] verify the existence of such a state.

<sup>16</sup>R. N. Barnett, U. Landman, and A. Nitzan, *J. Chem. Phys.* (to be published).